Journal of Food Measurement and Characterization (2023) 17:1515–1525
https://doi.org/10.1007/s11694-022-01726-2

ORIGINAL PAPER

Physicochemical and antimicrobial properties of biodegradable films based on gelatin/guar gum incorporated with grape seed oil

Neslihan Mutlu[1]

Received: 8 September 2022 / Accepted: 23 November 2022 / Published online: 2 December 2022

Abstract

This research has evaluated the effects of different levels (0.5, 1, and 1.5%) of grape seed oil (GSO) on the various aspects of gelatin/guar gum (GG) based biodegradable films. Bovine gelatin and GG-based biodegradable films incorporated with cold press GSO were prepared through the casting technique. With the increase of GSO concentration tensile strength (TS) (8.32–6.54 MPa), water vapor permeability ($4.80–2.65 \times 10^{-10}$ g mm/m^2 h Pa), moisture content (MC) (17.52–15.01%), and solubility in water (36.52–27.25%) decreased significantly ($p < 0.05$). Structural (SEM, XRD), chemical (FTIR), thermal (DSC), antibacterial properties, and color parameters of films were also investigated. SEM images proved a uniform structure in the gelatin/GG film surface. The incorporation of GSO into the films led to the formation of a slightly porous structure. Total color difference (ΔE) also increased with the level of incorporated GSO ($p < 0.05$). XRD analysis of films demonstrated a typical semi-crystalline structure. When GSO was incorporated into the film matrix the melting point (T_{max}) increased. The gelatin/GG/GSO films showed improved antimicrobial activity against tested both Gram-negative and Gram-positive bacteria. The biological properties of gelatin/GG/GSO films make them a promising material to prevent food spoilage for use in food packaging.

Keywords Antimicrobial · Biodegradable film · Gelatin film · Grape seed oil · Guar gum

Introduction

Increasing consumer awareness of food safety, quality, health, nutrition, and environmental issues has led companies and researchers to improve their productivity to develop sustainable films and coatings suitable for packaging applications [1–3]. Besides, the most commonly used polymers in packaging are derivated from petroleum products, and these non-biodegradable products lead to serious environmental problems [4]. Hence, nowadays, biodegradable, edible, nontoxic, and renewable coatings made from a biopolymer, such as proteins, polysaccharides, and fats used alone or in combination, have gained more significance [1, 5, 6].

Gelatin is one of the most important sources of biodegradable films and is regarded as a special and unique hydrocolloid [7, 8]. Gelatin is a protein obtained by hydrolysis of collagen gained from the skin, bone, or tissues of animals [9–11]. Gelatin-based films generally are superior to polysaccharide-based films due to their high gas barrier, high transparency, film-forming ability, and low cost [12]. However, due to the hydrophilic nature of gelatin, poor mechanical and water barrier properties of neat gelatin-based films could limit their application as packaging material [13, 14]. As a solution, crosslinking with other polysaccharides, such as natural gums, has been made to modify the thermal and mechanical properties of gelatin and has recently been explored [15, 16]. Intermolecular interactions, such as strong bonds via hydrophobic–hydrophobic and/or electrostatic interactions, in a polymeric network of polysaccharides and proteins could enhance the physical, mechanical, and barrier properties of protein-polysaccharide films [13].

Guar gum is obtained from the guar bean plant and is composed of a galactomannan sugars chain (galactose and mannose). There are four major sources of seed galactomannans: locust bean, guar, tara, and fenugreek, and they are hydrophobic compounds. Among these, only locust bean and GG are of considerable industrial importance due to their availability and price; hence it is primarily investigated by a number of researchers as a source of galactomannan [17,

✉ Neslihan Mutlu
n.mutlu@kafkas.edu.tr

[1] Department of Biology, Faculty of Arts and Sciences, Kafkas University, Kars, Turkey

18]. GG is a well-known polysaccharide in the food industry for its natural thickener, emulsifier, and stabilizer characteristics [19, 20] and guaranteeing the biodegradability and edibility of products containing GG. The effortless solubility of GG in cold or hot water to form a highly viscous solution effortless at low concentrations tend to its strong hydrogen bonding properties [19, 21, 22]. The physical properties of GG depend on the average galactose content, and its strong interactions with biopolymers can be observed with lower galactose content [18]. Due to its non-ionic character, the properties of guar gum are not affected by ionic strength and pH values at moderate temperatures [23].

In order to remove deficiencies of biodegradable films, such as low mechanical and water barrier properties, adding hydrophobic compounds such as lipids is also one of the effective approaches. Adding essential oils (EOs) into the film matrix prevents moisture transport due to their low polarity and hydrophobicity [24, 25]. EOs are volatile compounds obtained from plants, and they can be used in foods due to their non-toxic nature, organoleptic, biological, and therapeutic properties, and functional effects such as anti-oxidation and antimicrobial activity [26, 27]. Microbial contamination of foods is a serious concern to human health. Traditional methods, such as antimicrobial dips and sprays, have had limited success, and biopolymer films may be a new approach to overcome these limitations [28]. It has been reported that plant-based EOs as antimicrobial agents have successfully been incorporated into biodegradable films and enhanced film's antimicrobial, antioxidant, and physicochemical properties. EOs and extracts of different parts of plants (fruits, leaves, and seeds) incorporated into biodegradable films as antimicrobial agents control microbial growth on the surface of foods, increasing the shelf-life and quality of products [29, 30]. However, studies on the effect of EO incorporation into gelatin/GG-based films on the physicochemical and antimicrobial properties of the films are limited.

Among the various EOs, GSO is very popular for consumption due to its nutraceutical properties and contains vitamin E, unsaturated fatty acids (UFAs), and phytosterols. Linoleic acid is the main fatty acid associated with numerous health benefits, and α-tocopherol is the main tocopherol homolog of GSO [31, 32]. Cold-pressed GSO is a suitable alternative to other commonly used vegetable oils because of its higher amounts of essential fatty acids, and many other bioactive compounds, and it is an eco-friendly oil as it is a by-product of wine and grape juice-making processes [33]. Information on the antimicrobial properties of GSO is limited. A recent study reported that GSO inhibited the growth of *Staphylococcus aureus* and *Candida albicans* [31].

As far as we know, there is no detailed research in the literature that addresses the effects of GSO on the characteristics of the gelatin/GG films. Therefore, the main target of this research was to study the influence of GSO at different concentrations in the gelatin/GG-based biodegradable films. For this purpose, the resulting gelatin/GG/GSO films have been investigated for their physicochemical and antimicrobial properties. The incorporation with GSO will improve the film's physical, mechanical, and antimicrobial properties as food packaging.

Materials and methods

Materials

Bovine gelatin (bloom 200) and GG powder were purchased from Kimbiotek Co. (Istanbul, Turkey), and cold-press GSO was purchased from Arifoğlu Co. (Istanbul, Turkey), respectively, and were used without purification. Tween 80 and liquid glycerol were provided by Sigma Aldrich Chemie Gmbh (Darmstadt, Germany). Nutrient Broth and Mueller–Hinton Agar were supplied by Oxoid Ltd. (Basingstoke, UK). The bacteria strains (*Escherichia coli* ATCC 35218 *Escherichia coli* O157:H7 RSSK 09007, *Pseudomonas aeruginosa* ATCC 27853, *Staphylococcus aureus* ATCC 29213) were obtained from the Laboratory of Microbiology, Biology Department, Kafkas University (Turkey). All chemical reagents and materials used in this study were of analytical grade.

Film preparation

Films were prepared by casting technique. 5% (w/v) food-grade gelatin hydrated in distilled water at 20 °C to 25 °C for 30 min, then heated on a magnetic stirrer until it reached 50 °C. After that 0.5% (w/v) GG was added to the gelatin solution and stirred for 1 h at 60 °C. Glycerol (40% based on g gelatin) as a plasticizer and Tween 80 (0.2% based on mL GSO) as an emulsifier were added to the solution under constant stirring for 1 h. Then GSO at different concentrations (0.5, 1, and 1.5% v/v) were added to the solution and the film solution homogenized at 13,000 rpm for 3 min at room temperature using a homogenizer (Wiggenhauser, D-130, Germany). The resulting solution was mixed slowly with a low speed of stirring for 30 min to remove the air bubbles. Then 25 mL film-forming solution was cast onto the polystyrene Petri dishes (9 cm in diameter) and dried at room temperature for 48 h. After drying, the films were peeled off and placed in a desiccator containing saturated magnesium nitrate at 25 °C with a relative humidity of 50 ± 3% for 48 h before analysis. Films were produced without GSO and Tween 80 as control.

Characterization of films

Film thickness and mechanical properties

The thickness of the film samples was measured by using a digital micrometer (Loyka, 5203, Ankara, Turkey). The measurements were performed with the 1 µm precision in 5 points equally distributed around the circle 10 mm from its edge. The average value of these estimations was accepted as the film thickness.

The tensile strength and EAB of the films were calculated using a texture analyzer (Testform / AS1, Ankara, Turkey) according to the methodology described by Khodaman et al. [5]. The films were cut into 6 cm × 1 cm strips. Initial grip separation was 40 mm/min and crosshead speed was 50 mm/min. TS (MPa) and EAB (%) were measured by the texture analyzer device. Three repetitions were carried out for each film sample.

Colorimetric measurements

The color of the films was determined by spectrophotometer (X-Rite Ci7800, Michigan, USA). Film specimens were placed on a white standard plate (L* = 95.69, a* = − 0.37, and b* = 2.14), and CIELAB color coordinates, L (lightness), a (red-green), and b (yellow-blue) values were measured. Additionally, the DL*, Da*, and Db* values of the film samples containing GSO were also measured and compared with the control group, where DL* is negative for darker, Da* is positive for redder, and Db* is negative for bluer. The color difference (ΔE) was calculated using Eq. (1):

$$\Delta E = \sqrt{(L - L^*)^2 + (a - a^*)^2 + (b - b^*)^2} \quad (1)$$

where L*, a*, and b* are the color parameter values of the standard plate and L, a, and b are the color parameter values of the sample.

Moisture content

Pieces of each film (2 cm × 2 cm) were cut and weighed, then dried at 105 ± 1 °C in a laboratory oven until they reached constant weight. Moisture content (MC) was determined using Eq. (2):

$$MC(\%) = \frac{m_1 - m_2}{m_1} \times 100 \quad (2)$$

where m_1 and m_2 are the initial and the dried sample weight, respectively.

Water vapor permeability (WVP)

Water vapor permeability measures film resistance to water vapor. WVP was measured using the standard ASTM method E96 [34]. Cups with a diameter 2 cm and a depth of 5 cm were used. After placing 3 g anhydrous calcium chloride (RH = 0%) in each cup, films were covered on the top of the cups. The weighing cups were put into a desiccator containing sodium chloride saturated solution (R = 75%) at 25 °C. Cups were weighed every 24 h for 3 days and the water vapor transmission rate (WVTR) was calculated by the weight gain of the cup. Changes in the weight of the cups were plotted as a function of time. After that slope was obtained by the linear regression from the weight and time changes. WVTR and WVP were calculated using Eqs. (3) and (4):

$$WVTR = \frac{\Delta m}{Ax\Delta t} \quad (3)$$

$$WVP = \frac{\mathrm{WVTR}xx}{\Delta \mathrm{P}} \quad (4)$$

where Δm is the change in weight over time (t), A is the surface area of the exposed film, x is film thickness, and ΔP is the difference in partial pressure.

Water solubility (WS)

The solubility (%) of films was determined by the following method: the film samples were cut to 3 cm × 3 cm weighed, and then immersed in 50 mL distilled water for 24 h at room temperature with low-speed stirring. The dry weight of the remaining film pieces was obtained after filtration on previously dried and weighed filter paper and used to calculate the insoluble matter as a percentage of the initial dry weight. The film pieces remaining on the filter paper were dried in the oven at 105 °C for 24 h [4]. The solubility (%) of the film sample was calculated using Eq. (5):

$$WS(\%) = \frac{\text{Initial} - \text{final weight}}{\text{Initial weight}} \times 100 \quad (5)$$

X-ray diffraction (XRD) analysis

X-ray diffraction patterns of films were analysed using an X-ray diffractometer (Bruker AXS D8 Advance, Madison, WI, USA) operated at 42 kV, 30 mA, and 1.540 A°, and spectra were recorded using CuKa radiation. Distribution patterns were obtained at 2θ angles, 5 to 60 °C at room temperature (25 °C) [35].

Fourier-transform infrared (FTIR) analysis

The FTIR spectra were used to determine the specific absorption bands of the films. FTIR spectra were recorded at room temperature with 18 scans per sample on a Thermo Fisher Nicolet i50 in the range of 4000–500 cm^{-1}. The resolution was monitored at 32 cm^{-1} [36].

Differential scanning calorimetry (DSC) analysis

The thermal properties of the films were determined by a differential scanning calorimetry device (TA/Discovery DSC250, New Castle, USA). The samples (1 cm × 1 cm) were put in the device and heated to 10 °C/min at a temperature of − 20 to 150 °C under the nitrogen flow (50 mL/min) [36].

Scanning electron microscopy (SEM)

In order to investigate the surface morphology of films, SEM (Carl Zeiss Gemini 300, Germany) images were used. Briefly, film samples (2 cm × 2 cm) were coated with gold using a vacuum before observation. The samples were placed on the specimen holder and examined using a low vacuum at a voltage of 15 kV [24].

Antimicrobial properties

The antimicrobial activity of the neat gelatin/GG and GSO-loaded gelatin/GG films was determined by the disc diffusion method against both Gram-negative (*Escherichia coli*) and Gram-positive (*Staphylococcus aureus* and *Pseudumonas aeruginosa*) bacteria. Microorganisms used for the test were incubated in Mueller–Hinton Agar at 37 °C for 24 h. Then, colonies were transferred into sterile saline, and the turbidity of bacterial suspension was adjusted to 0.5 MacFarland (1.5×10^8 CFU/mL). Sterile swabs were used to spread suspension on Mueller–Hinton Agar. Film samples (15 mm × 15 mm) were placed on an agar plate and incubated at 37 °C for 24 h. The diameter of the inhibition halo (mm) around the film samples was measured with three replications, and its average was reported [15].

Statistical analysis

For statistical analysis of the characteristics of the film, each factor was presented as the mean ± standard deviation. One-way ANOVA and Tukey (SPSS, version 22, Chicago, IL) tests were used to compare the differences among mean values at a 5% significant level.

Results and discussion

Film characterization

Film thickness, mechanical properties, MC, WVP, and WS

Film thickness affects the mechanical properties of films. Table 1 presents the properties of thickness, TS (MPa) and EAB (%), MC (%), WVP, WS (%), and color of the films. The thickness of the film depends on biopolymers, emulsifiers, plasticizers, and active components such as EOs [37]. According to the results, incorporating GSO at 1 and 1.5% concentrations increased the film thickness significantly due to the increase in the film solution.

One of the important parameters in increasing the shelf life of food and limiting the activity of microorganisms is the moisture content of biodegradable films [35]. The hydrophobicity of the films was increased, and moisture content decreased by adding GSO at concentrations of 1 and 1.5%. Interactions between oil components and some hydrophilic domains of protein could promote a decrease in the hydrophobic character of the film matrix [38]. However, incorporating a lower concentration of GSO (0.5%) did not affect the moisture content significantly ($p > 0.05$). The highest moisture content value was obtained for gelatin/GG film due to the hydrophilic character of gelatin, GG, and glycerol. Incorporating GSO decreased the moisture content of films in different proportions, similar to the results obtained for

Table 1 Physical properties of films

	Control (Gelatin/GG)	Gelatin/GG/0.5% GSO	Gelatin/GG/1% GSO	Gelatin/GG/1.5% GSO
Thickness (mm)	0.2486 ± 0.006^{c}	0.2416 ± 0.013^{d}	0.2652 ± 0.004^{b}	0.315 ± 0.006^{a}
Moisture content (%)	17.52 ± 0.40^{a}	17.49 ± 0.05^{a}	15.26 ± 0.23^{b}	15.01 ± 0.08^{b}
Water Solubility (%)	36.52 ± 0.81^{a}	35.37 ± 0.63^{a}	28.48 ± 0.46^{b}	27.25 ± 0.19^{b}
WVP ($\times 10^{-10}$ g mm/m^2 h Pa)	4.80 ± 0.06^{a}	3.70 ± 0.12^{b}	3.04 ± 0.12^{c}	2.65 ± 0.05^{d}
TS (MPa)	8.32 ± 1.08^{a}	7.26 ± 0.20^{ab}	6.63 ± 0.65^{b}	6.54 ± 0.31^{b}
EAB (%)	92.37 ± 10.09^{a}	89.77 ± 4.09^{a}	104.44 ± 5.27^{a}	106.62 ± 6.19^{a}

Means within each row with the same letters are not significantly different ($p < 0.05$). Data are mean ± SD

gelatin/palm oil [39], gelatin/nano-ZnO/*Mentha piperita* EO [40], and pectin/glove EO [41].

Water vapor permeability describes a film's ability to allow water vapor to pass through the matrix and prevent moisture transfer between food and the environment. It is one of the most important parameters because moisture plays an important role in food spoilage, so it should be as low as possible [15]. Gelatin/GG film has high water permeability due to its hydrophilic feature. However, as seen in Table 1, adding GSO shifted WVP values significantly ($p < 0.05$) at all added concentrations. This may be explained by the interactions between the biopolymeric network and the EOs, which reduces the availability of the hydroxyl groups to interact with the water [37]. Furthermore, WVP depends on the hydrophilic-hydrophobic ratio of film components [42]. Similar results were observed for thyme EO incorporated hake protein-based films [43], different oils (peanut oil, corn oil, salad oil, and cod live oil) incorporated fish water-soluble proteins [44], and bergamot, kaffir lime, lemon, and lime EOs incorporated fish skin gelatin [45]. In contrast, Kavoosi et al. [46] showed an increase in the WVP values of gelatin films (10% w/v) due to the addition of *Zataria multofida* EO at different concentrations (2, 4, 6, and 8% of gelatin). Altiok et al. [47] and Nunes et al. [48] also reported similar results. Results may vary due to the oil concentration of films, which causes the formation of a porous structure and the increase of WVP value and/or the nuances of emulsion preparation steps such as homogenization and drying processes.

Table 1 summarized the WS (%) of the gelatin/GG films. The gelatin /GG film presented a solubility percentage of $36.52 \pm 0.81\%$, but with the incorporation of the GSO, there was a decrease in the solubilities of the films to $27.25 \pm 0.19\%$. Non-polar components of oil interacted with the hydrophobic domains of gelatin, leading to the increase in hydrophobicity of the resulting film. As a result, the solubility of the film was lowered [38]. Martucci et al. [49] observed a reduction in the water content of gelatin film with the addition of lavender oil, and Jamroz et al. [50] and Wu et al. [51] reported a decrease in film solubility by adding oil.

The mechanical properties of films are a crucial factor in the quality of food products during transportation and storage. TS and EAB describe the mechanical resistance of films, which should be as high as possible [24]. TS value demonstrates the maximum tensile stress that film can endure, and EAB shows the maximum change in length of film before breaking [10]. TS and EAB of gelatin/GG films incorporated with GSO at different levels are shown in Table 1. When compared with the control film (gelatin/GG), films added with GSO (0.5–1.5%) showed a significantly reduced TS ($p < 0.05$). Many works have reported a decrease in TS as lipid concentration increases in films based on polysaccharides [4, 10, 52, 53]. This behaviour can be attributed to a decrease in the interaction between the gelatin molecules, leading to a less cohesive structure and an increase in the flexible domains within the film [54, 55]. The effects of destabilization phenomena during the film drying were also considered [4]. Gelatin/GG films with or without GSO exhibited similar and high EAB values. Oil addition may affect the flexibility of films depending on the characteristic of the oil added. Many previous studies reported that films incorporated with active compounds such as oils showed EAB value increase directly proportional to the added oil level, which is in accordance with our results [43, 54–56].

Color properties

Color is one of the important factor affecting product appearance and consumer preference. Table 2 shows the color parameters of films. Also, Fig. 1 shows the appearances of films. As shown in Fig. 1, gelatin/GG film without GSO is more transparent than films with GSO. As expected, when the GSO incorporated films compared with the control film, it was determined that the L value (lightness) decreased and the b value (yellow, blue) increased due to the yellowish color of GSO. Total color difference (ΔE) also increased ($p < 0.05$) with the level of incorporated GSO, and the highest ΔE was observed in the film containing the highest levels of GSO. Many previous studies have reported that adding EOs to biodegradable films causes significant color changes [57–59]. Biodegradable films should be as colorless as possible to simulate the commonly used synthetic polymers, so incorporating oil into the films may cause undesirable color changes [10].

Table 2 Color measurements

	L	a	b	ΔE	DL*	Da*	Db*
Gelatin/GG	92.83 ± 0.15^{a}	-1.48 ± 0.03^{c}	11.11 ± 0.05^{c}	9.57 ± 0.35^{d}	–	–	–
Gelatin/GG/0.5% GSO	91.49 ± 0.24^{b}	-1.28 ± 0.02^{b}	11.91 ± 0.02^{b}	10.69 ± 0.17^{c}	-1.34 ± 0.03^{a}	0.20 ± 0.04^{c}	0.71 ± 0.02^{b}
Gelatin/GG/1% GSO	90.84 ± 0.27^{c}	-1.15 ± 0.04^{a}	11.89 ± 0.01^{b}	11.83 ± 0.15^{b}	-1.40 ± 0.04^{a}	0.32 ± 0.05^{b}	0.74 ± 0.02^{b}
Gelatin/GG/1.5% GSO	89.81 ± 0.21^{d}	-1.07 ± 0.06^{a}	14.70 ± 0.1^{a}	13.61 ± 0.46^{a}	-2.42 ± 0.11^{b}	0.58 ± 0.06^{a}	3.57 ± 0.17^{a}

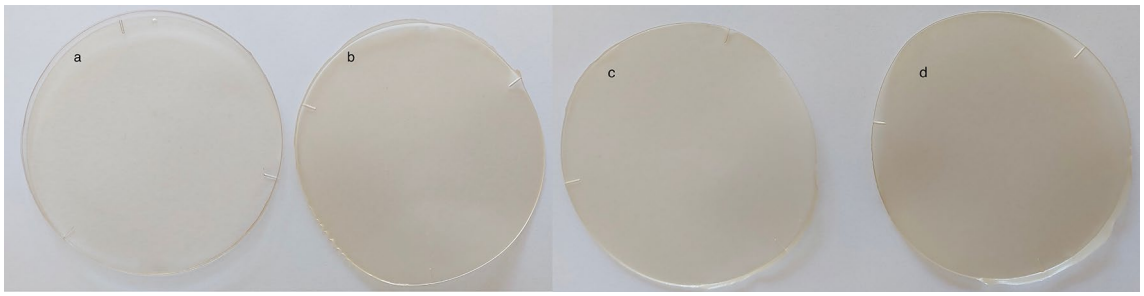

Fig. 1 Photographs of the gelatin/GG/GSO films: **a** film without GSO, **b** loaded with 0.5% (w/w) GSO, **c** loaded with 1.0% (w/w) GSO, and **d** loaded with a 1.5% (w/w) GSO

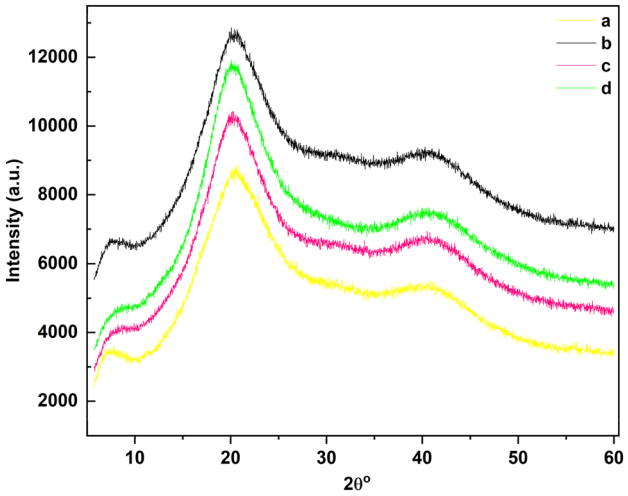

Fig. 2 X-ray diffraction diagram of **a** film without GSO, **b** loaded with 0.5% (w/w) GSO, **c** film loaded with 1.0% (w/w) GSO, and **d** film loaded with a 1.5% (w/w) GSO

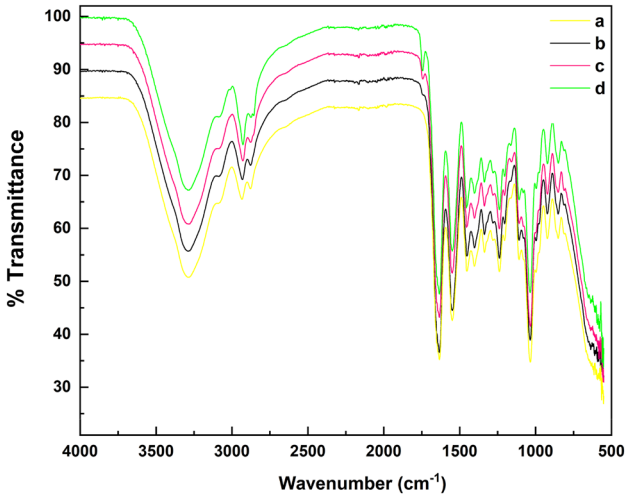

Fig. 3 FTIR spectra of **a** film without GSO, **b** film loaded with 0.5% (w/w) GSO, **c** film loaded with 1.0% (w/w) GSO, and **d** film loaded with a 1.5% (w/w) GSO

X-ray diffraction (XRD) analysis

The XRD patterns of gelatin/GG, gelatin/GG/0.5% GSO, gelatin/GG/1% GSO, and gelatin/GG/1.5% GSO films are depicted in Fig. 2. All designated gelatin/GG-based films exhibited two characteristic peaks around 2θ= 8° and 2θ= 20 implying the semi-crystalline structure of the biopolymer [61]. Peaks around 2θ= 20 indicate the presence of characteristic peaks of the polymer chain of GG and gelatin. [19]. Neat gelatin/GG film revealed two peaks at 2θ= 7.6 and 2θ= 20.61° according to the α-helix and β-sheet structures of the gelatin [62]. The humps in the bands of films show GG's little crystalline behavior compared to gelatin [19]. The peaks of gelatin/GG-based films insignificantly shifted due to the incorporation of GSO. Peaks of films incorporated with GSO at concentrations 0.5, 1, and 1.5% decreased to 2θ of 20.16°, 20.43°, and 20.26°, respectively. According to the results of previous studies, it has been reported that the characteristic peak is around 2θ=20° in gum-based films [24], neat gelatin films, and gelatin/gum films [13]. By incorporating GSO, no significant effect was observed. In accordance with our observations, some studies have shown that EO incorporation does not have a significant effect on the crystallinity of gelatin-based films [26, 63].

Fourier transform infrared (FTIR) analysis

The FTIR spectra of films were identified as shown in Fig. 3 Gelatin/GG film designated peaks at 3248.98^{-1}, 2933.90^{-1}, 1633.26^{-1}, 1548.53^{-1}, and 1238.25^{-1}, which indicates the amide bands consisted of amide A (representing the NH-stretching coupled with hydrogen bonding), amide B (illustrating the CH stretching and $-NH_3^+$), amide I (illustrating C=O stretching and hydrogen bonding coupled with COO), amide II (presenting the bending vibrations of N–H groups and stretching vibrations of C–N groups), and amide III (indicating the vibrations in-plane of C–N and N–H groups of bound amide), respectively. The presence of these bands is due to the vibrational motions of the peptide bonds of the amino acids of gelatin and GG [61, 64]. The peak at

1034.05^{-1} corresponds to the interactions between the film structure and the OH group of glycerol added as a plasticizer [65]. FTIR spectra of gelatin/GG and gelatin/GG containing GSO films exhibited similar characteristic main peaks, but the amplitudes of the peaks varied, which may be related to the presence of terpene-protein interactions between GSO and gelatin/GG [38]. The amplitude of two peaks at wavenumbers around 2850^{-1} and 2950^{-1} increased when the films were incorporated with GSO and these peaks represent the methylene asymmetrical and symmetrical stretching vibration of the aliphatic C–H in CH_2 and CH_3 groups, respectively [45]. A tiny peak at a wavenumber of 1744.22^{-1} was found in gelatin/GG enriched with GSO (0.5, 1, and 1.5%) film, corresponding to the C=O stretching vibration of the aldehyde or ester carbonyl groups of GSO [66]. There was no peak at around 1744^{-1} in gelatin/GG film. Incorporating with GSO may increase the hydrophobicity of gelatin/GG films and it was supported by the WVP results.

Differential scanning calorimetry (DSC) analysis

The thermal stability of films was determined by DSC. Figure 4 shows the typical DSC thermogram of gelatin films with or without GSO. For endothermic/melting transition, the control film exhibited the endothermic peak at a temperature (T_{max}) of 61.44 °C, attributed to the melting of the triple-helix crystalline structure of gelatin [67]. When GSO was incorporated into the film matrix, the T_{max} peak became broader and slightly increased. The control film showed the lowest ΔH, compared with others. Films incorporated with GSO required a higher enthalpy for disruption of the interchain interaction. Interestingly, when the gelatin/GG/GSO films were compared, the T_{max} temperature was the highest in the films incorporating 0.5% GSO, while this temperature was the lowest in the films incorporating 1.5% GSO as in the ΔH values. A high amount of EOs incorporated might increase the amorphous phase with the concomitant decrease in the ordered phase and thus increase molecular mobility [54], and the lipid droplet size or distribution of the films may cause this non-gradual increase.

Film morphology

The surface of gelatin/GG control film was compact, uniform and smooth without pores or cracks (Fig. 5). Continuous structure with no cracks in films was observed in the surface images of films without and with GSO. As seen in the images, the migration of oil droplets to the surface of the polysaccharide network causes holes in the surface of oil-containing films, which is due to the hydrophobic nature of the oil. The results are in line with a report of previous studies [68, 69]. Different oils may participate in film structure and affect morphology differently [54]. Unexpectedly, the distribution of oil droplets in films containing 1.5% GSO was observed more homogeneously than in films containing 0.5% and 1% GSO. This observation is in line with a report by Ma et al. [67]. They declared the lipid droplet distribution in the gelatin film with 20% olive oil was more homogenous than those of gelatin films with 10% or 15% olive oil. This indicates that the microstructure (droplet size) of the films is related to the oil stability during the drying process [67].

Antimicrobial properties

Table 3 and Fig. 6 show the antimicrobial activities exhibited by the disc diffusion agar method against *E.coli, S.aureus, and P.aeruginosa*. According to the results obtained, gelatin/GG film without GSO showed no activity against the tested bacteria. Gelatin/GG/GSO films are effective against both Gram-positive and Gram-negative bacteria, while they are more effective against Gram-positive bacteria rather than against Gram-negative bacteria. This may be due to the more complex bilayer membrane of Gram-negative bacteria. Results indicated that GSO had higher antimicrobial activity against *S.aureus* than other species at all concentrations. EOs contains terpenoids, terpenes, and other aromatic and aliphatic compounds [60]. Phenolic compounds in EOs attack cell membrane phospholipids, thereby increasing permeability. In addition, phenolic compounds in EOs react with enzymes in the cell wall and cause cell membrane damage [40].

The antimicrobial activity displayed by phenolic compounds such as resveratrol in GSO is due to the induction of oxidative damage in the bacterial membrane, especially *E.coli,* without affecting the host cells [32]. It is extremely important that our results show that films incorporating 1.5% GSO can also be effective against Gram-negative bacteria such as *E.coli* O157:H7, which are more resistant to EOs than Gram-positive bacteria and are threat for food safety. GSO has the potential to be used for new and green packaging systems due to its high antibacterial property. Many studies have previously reported that EO incorporation into polysaccharide-based films activates the film and enhances the antimicrobial properties [38, 46, 47].

Conclusion

In this study, different concentrations of GSO were incorporated into gelatin/GG-based films to prepare antimicrobial films using the casting method and the effects of GSO on the properties of the films were investigated. Incorporating GSO into gelatin/GG films increased film thickness, leading to better water vapor barrier properties. The cross-linking between gelatin and GG provided more compact films. WS (%) properties of resulting gelatin/GG/GSO

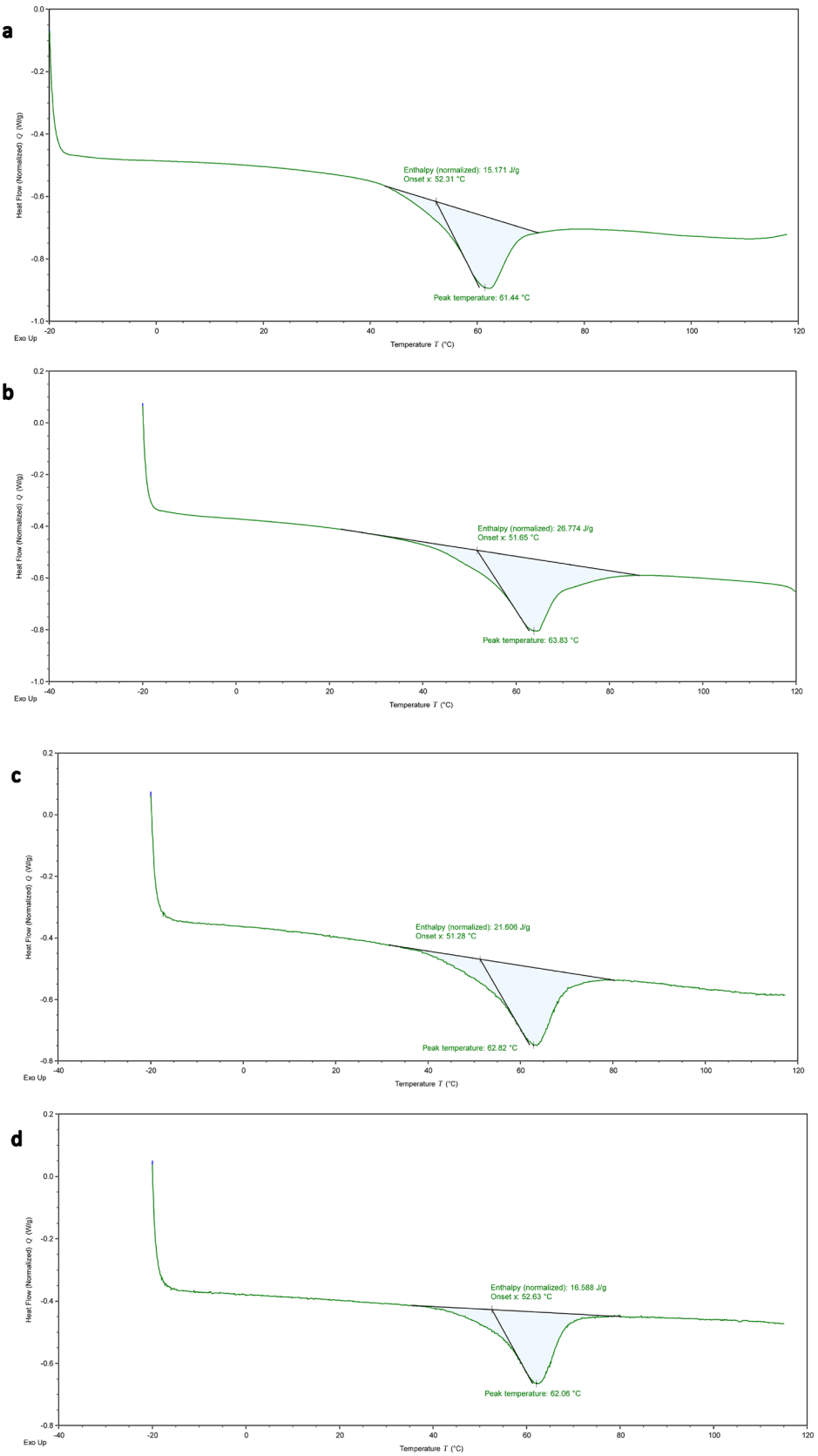

Fig. 4 DSC thermograms of **a** film without GSO, **b** film loaded with 0.5% (w/w) GSO, **c** film loaded with 1.0% (w/w) GSO, and **d** film loaded with a 1.5% (w/w) GSO

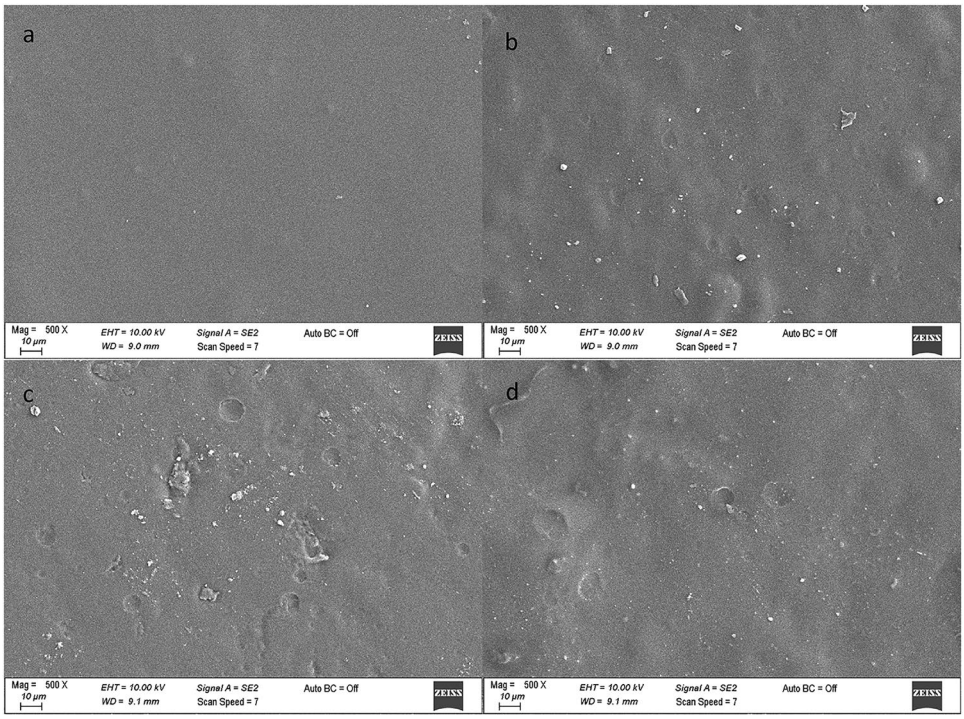

Fig. 5 SEM images of film surfaces **a** film without GSO, **b** film loaded with 0.5% (w/w) GSO, **c** film loaded with 1.0% (w/w) GSO, and **d** film loaded with a 1.5% (w/w) GSO

Table 3 Antimicrobial activity of biodegradable films

Strains	Zone of inhibition (mm)			
	Gelatin/GG	Gelatin/GG/0.5% GSO	Gelatin/GG/1% GSO	Gelatin/GG/1.5% GSO
S.aureus (ATCC 29213)	–	1.14 ± 02	3.20 ± 0.8	4.05 ± 0.9
P.aeruginosa (ATCC 27853)	–	–	–	3.02 ± 1.6
E.coli (ATCC 35218)	–	–	–	1.82 ± 0.3
E.coli O157:H7 (RSSK 09007)	–	–	1.12 ± 0.5	3.5 ± 1.2

Data are expressed as mean ± SD

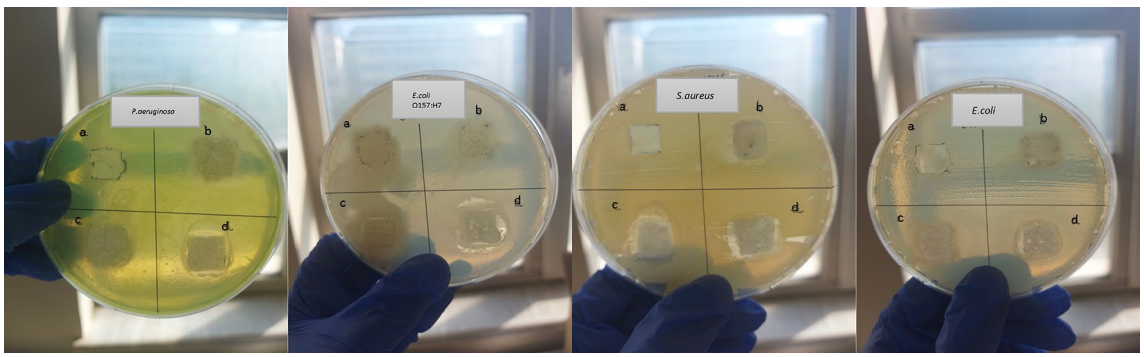

Fig. 6 Disc diffusion plates of **a** film without GSO, **b** film loaded with 0.5% (w/w) GSO **c** film loaded with 1.0% (w/w) GSO and **d** film loaded with a 1.5% (w/w) GSO

films decreased. Thermal properties of gelatin/GG/GSO films were influenced by the oil incorporated, and T_{max} peaks of films increased. High EAB values of more than 89% were determined, giving them a plastic material characteristic. The GSO favored the mechanical properties with a decrease in the TS. Continuous structure with no cracks in films was observed in the surface images of films without or with GSO. Importantly, the antimicrobial property of gelatin/GG-based films has been improved using GSO. GSO incorporated films inhibited the growth of *E.coli* O157:H7, *S.aureus, and P.aeruginosa.* These results indicate that biodegradable gelatin/GG films containing GSO present good potential for their utilization as antimicrobial active packaging material. Nevertheless, further studies are required to evaluate their performance in different types of foodstuffs.

Acknowledgements I would like to thank the staff at Bursa Technical University Central Research Laboratory for their technical assistance for SEM, XRD, DSC, FTIR, and tensile analysis. I thank Dr. Hüseyin Ertap for his help in graphic design.

Funding The authors declare that no funds, grants, or other support were received during the preparation of this manuscript.

Data availability The datasets generated during and/or analysed during the current study are available from the corresponding author on reasonable request.

Declarations

Competing ınterests The authors have no relevant financial or non-financial interests to disclose.

References

1. E. Tavassoli-Kafrani, H. Shekarchizadeh, M. Masoudpour-Behabadi, Carbohydr. Polym. (2016). https://doi.org/10.1016/j.carbpol.2015.10.074
2. P.J.P. Espitia, W.X. Du, R. de Jesús Avena-Bustillos, N.D.F.F. Soares, T.H. McHugh, Food hydrocoll. (2014). https://doi.org/10.1016/j.foodhyd.2013.06.005
3. A. Mehdizadeh, S.A. Shahidi, N. Shariatifar, M. Shiran, A. Ghorbani-HasanSaraei, J. Food Meas. Charact. (2022). https://doi.org/10.1007/s11694-021-01250-9
4. M.A. Oliveira, M.L. Gonzaga, M.S. Bastos, H.C. Magalhães, S.D. Benevides, R.F. Furtado, R.A. Zambelli, D.S. Garruti, Food Packag. Shelf Life (2020). https://doi.org/10.1016/j.fpsl.2019.100431
5. E. Khodaman, H. Barzegar, A. Jokar, H. Jooyandeh, J. Food Meas. Charact. (2022). https://doi.org/10.1007/s11694-022-01470-7
6. M. Gomaa, A.F. Hifney, M.A. Fawzy, K.M. Abdel-Gawad, Food Hydrocoll. (2018). https://doi.org/10.1016/j.foodhyd.2018.03.056
7. S. Sahraee, J.M. Milani, B. Ghanbarzadeh, H. Hamishehkar, Food Sci. Nutr. (2020). https://doi.org/10.1002/fsn3.1424
8. A.A. Karim, R. Bhat, Trends Food Sci. Technol. (2008). https://doi.org/10.1016/j.tifs.2008.08.001
9. A. Etxabide, V. Coma, P. Guerrero, C. Gardrat, K. de la Caba, Food Hydrocoll. (2017). https://doi.org/10.1016/j.foodhyd.2016.11.036
10. M.D. Khah, B. Ghanbarzadeh, L.R. Nezhad, A. Ostadrahimi, Int. J. Biol. Macromol. (2021). https://doi.org/10.1016/j.ijbiomac.2021.01.020
11. A.A. Tyuftin, J.P. Kerry, Food Packag. Shelf Life (2021). https://doi.org/10.1016/j.fpsl.2021.100688
12. J.F. Martucci, R.A. Ruseckaite, Polym. Plast. Technol. Eng. (2010). https://doi.org/10.1080/03602551003652730
13. M. Soltanzadeh, S.H. Peighambardoust, B. Ghanbarzadeh, S. Amjadi, M. Mohammadi, J.M. Lorenzo, H. Hamishehkar, Food Hydrocoll. (2022). https://doi.org/10.1016/j.foodhyd.2022.107620
14. J. Guo, L. Ge, X. Li, C. Mu, D. Li, Food Hydrocoll. (2014). https://doi.org/10.1016/j.foodhyd.2014.01.026
15. L. Yavari Maroufi, M. Ghorbani, M. Tabibiazar, Food Bioprocess Technol. (2020). https://doi.org/10.1007/s11947-020-02509-7
16. L. Nuvoli, P. Conte, C. Fadda, J.A.R. Ruiz, J.M. García, S. Baldino, A. Mannu, Polymer (2021). https://doi.org/10.1016/j.polymer.2020.123244
17. V.D. Prajapati, G.K. Jani, N.G. Moradiya, N.P. Randeria, B.J. Nagar, N.N. Naikwadi, B.C. Variya, Int. J. Biol. Macromol. (2013). https://doi.org/10.1016/j.ijbiomac.2013.05.017
18. G. Sharma, S. Sharma, A. Kumar, H. Ala'a, M. Naushad, A.A. Ghfar, G.T. Mola, F.J. Stadler, Carbohydr. Polym. (2018). https://doi.org/10.1016/j.carbpol.2018.07.053
19. N. Khan, D. Kumar, P. Kumar, Colloids Interface Sci. Commun. (2020). https://doi.org/10.1016/j.colcom.2020.100242
20. S. Ramazani, M. Rostami, M. Raeisi, M. Tabibiazar, M. Ghorbani, Food Hydrocoll. (2019). https://doi.org/10.1016/j.foodhyd.2018.12.010
21. N.M. Oliveira, F.Q. Dourado, A.M. Peres, M.V. Silva, J.M. Maia, J. Teixeira, Food Bioprocess Technol. (2011). https://doi.org/10.1007/s11947-010-0324-6
22. R.A. Rub, S. Sasikumar, Arab J. Chem. (2016). https://doi.org/10.1016/j.arabjc.2012.04.012
23. P.K. Binsi, N. Nayak, P.C. Sarkar, C.G. Joshy, G. Ninan, C.N. Ravishankar, J. Food Sci. Technol. (2017). https://doi.org/10.1007/s13197-017-2496-9
24. R. Niknam, B. Ghanbarzadeh, H. Hamishehkar, Polym. Test. (2019). https://doi.org/10.1016/j.polymertesting.2019.04.015
25. A. Aydogdu, C.J. Radke, S. Bezci, E. Kirtil, Int. J. Biol. Macromol. (2020). https://doi.org/10.1016/j.ijbiomac.2019.12.255
26. Y. Shen, Z.J. Ni, K. Thakur, J.G. Zhang, F. Hu, Z.J. Wei, Int. J. Biol. Macromol. (2021). https://doi.org/10.1016/j.ijbiomac.2021.03.133
27. Y. Alparslan, J. Food Meas. Charact. (2018). https://doi.org/10.1007/s11694-017-9643-x
28. S. Benavides, R. Villalobos-Carvajal, J.E. Reyes, J. Food Eng. (2012). https://doi.org/10.1016/j.jfoodeng.2011.05.023
29. A. Mehdizadeh, S.A. Shahidi, N. Shariatifar, M. Shiran, A. Ghorbani-HasanSaraei, J. Aquat. Food Prod. Technol. (2022). https://doi.org/10.1080/10498850.2020.1855688
30. X. Zhang, B.B. Ismail, H. Cheng, T.Z. Jin, M. Qian, S.A. Arabi, D. Liu, M. Guo, Carbohydr. Polym. (2021). https://doi.org/10.1016/j.carbpol.2021.118616
31. N.M. Dabetic, V.M. Todorovic, I.D. Djuricic, J.A. Antic Stankovic, Z.N. Basic, D.S. Vujovic, S.S. Sobajic, Eur. J. Lipid Sci. Technol. (2020). https://doi.org/10.1002/ejlt.201900447
32. J. Garavaglia, M.M. Markoski, A. Oliveira, A. Marcadenti, Nutr. Metab. Insights (2016). https://doi.org/10.4137/NMI.S32910
33. F.B. Shinagawa, F.C.D. Santana, L.R.O. Torres, J. Mancini-Filho, Food Sci. Technol. (2015). https://doi.org/10.1590/1678-457X.6826
34. ASTM, Manual Book of ASTM Standard (2000)
35. A. Asdagh, I. Karimi Sani, S. Pirsa, S. Amiri, N. Shariatifar, H. Eghbaljoo-Gharehgheshlaghi, Z. Shabahang, A. Taniyan, J. Polym. Environ. (2021). https://doi.org/10.1007/s10924-020-01882-w

36. F. Chavoshi, Z. Didar, M. Vazifedoost, M. Shahidi Noghabi, A. Zendehdel, J. Food Meas. Charact. (2022). https://doi.org/10.1007/s11694-022-01533-9
37. C. Vilas Dhumal, K. Pal, P. Sarkar, J. Mater. Sci. Mater. Med. (2019). https://doi.org/10.1007/s10856-019-6317-8
38. M. Ahmad, S. Benjakul, T. Prodpran, T.W. Agustini, Food Hydrocoll. (2012). https://doi.org/10.1016/j.foodhyd.2011.12.003
39. P. Tongnuanchan, S. Benjakul, T. Prodpran, K. Nilsuwan, Food Hydrocoll. (2015). https://doi.org/10.1016/j.foodhyd.2015.02.025
40. S. Javidi, A. Mohammadi Nafchi, H.H. Moghadam, J. Food Meas. Charact. (2022). https://doi.org/10.1007/s11694-021-01217-w
41. T. Nisar, Z.C. Wang, X. Yang, Y. Tian, M. Iqbal, Y. Guo, Int. J. Biol. Macromol. (2018). https://doi.org/10.1016/j.ijbiomac.2017.08.068
42. L.M. Reyes, M. Landgraf, P.J.D.A. Sobral, Food Packag. Shelf Life (2021). https://doi.org/10.1016/j.fpsl.2020.100607
43. C. Pires, C. Ramos, G. Teixeira, I. Batista, R. Mendes, L. Nunes, A. Marques, J. Food Eng. (2011). https://doi.org/10.1016/j.jfoodeng.2011.02.036
44. M. Tanaka, S. Ishizaki, T. Suzuki, R. Takai, J. Tokyo Univ. Fish. **87**, 31–38 (2001)
45. P. Tongnuanchan, S. Benjakul, T. Prodpran, Food Chem. (2012). https://doi.org/10.1016/j.foodchem.2012.03.094
46. G. Kavoosi, A. Rahmatollahi, S.M.M. Dadfar, A.M. Purfard, LWT (2014). https://doi.org/10.1016/j.lwt.2014.02.008
47. D. Altiok, E. Altiok, F. Tihminlioglu, J. Mater. Sci. Mater. Med. (2010). https://doi.org/10.1007/s10856-010-4065-x
48. J.C. Nunes, P.T.S. Melo, M.V. Lorevice, F.A. Aouada, M.R. de Moura, J. Food Sci. Technol. (2021). https://doi.org/10.1007/s13197-020-04469-4
49. J.F. Martucci, L.B. Gende, L.M. Neira, R.A. Ruseckaite, Ind. Crops Prod. (2015). https://doi.org/10.1016/j.indcrop.2015.03.079
50. E. Jamróz, L. Juszczak, M. Kucharek, J. Appl. Polym. Sci. (2018). https://doi.org/10.1002/app.46754
51. J. Wu, H. Liu, S. Ge, S. Wang, Z. Qin, L. Chen, Q. Zheng, Q. Liu, Q. Zhang, Food Hydrocoll. (2015). https://doi.org/10.1016/j.foodhyd.2014.06.017
52. Q. Ma, L. Du, L. Wang, Sens. Actuators B Chem. (2017). https://doi.org/10.1016/j.snb.2017.01.035
53. L. Sánchez-González, M. Cháfer, A. Chiralt, C. González-Martínez, Carbohydr. Polym. (2010). https://doi.org/10.1016/j.carbpol.2010.04.047
54. P. Tongnuanchan, S. Benjakul, T. Prodpran, S. Pisuchpen, K. Osako, Food Hydrocoll. (2016). https://doi.org/10.1016/j.foodhyd.2015.12.005
55. M.H.R. Barbosa, S.D.A. Goncalves, L. Marangoni Junior, R.M.V. Alves, R.P. Vieira, J. Food Meas. Charact. (2022). https://doi.org/10.1007/s11694-022-01337-x
56. H. Abbasi, H. Fahim, M. Mahboubi, J. Food Meas. Charact. (2021). https://doi.org/10.1007/s11694-020-00799-1
57. W.X. Du, C.W. Olsen, R.J. Avena-Bustillos, T.H. McHugh, C.E. Levin, M. Friedman, J. Food Sci. (2009). https://doi.org/10.1111/j.1750-3841.2009.01282.x
58. Y.A. Arfat, S. Benjakul, T. Prodpran, P. Sumpavapol, P. Songtipya, Food Hydrocoll. (2014). https://doi.org/10.1016/j.foodhyd.2014.04.023
59. M. Ejaz, Y.A. Arfat, M. Mulla, J. Ahmed, Food Packag. Shelf Life (2018). https://doi.org/10.1016/j.fpsl.2017.12.004
60. A. Tügen, B. Ocak, Ö. Özdestan-Ocak, J. Food Meas. Charact. (2020). https://doi.org/10.1007/s11694-020-00547-5
61. Y. Shahbazi, N. Shavisi, N. Karami, R. Lorestani, F. Dabirian, LWT (2021). https://doi.org/10.1016/j.lwt.2021.112322
62. S. Amjadi, H. Almasi, B. Pourfathi, S. Ranjbaryan, J. Polym. Environ. (2021). https://doi.org/10.1007/s10924-021-02097-3
63. E.M.C. Alexandre, R.V. Lourenço, A.M.Q.B. Bittante, I.C.F. Moraes, P.J. do Amaral Sobral, Food Packag Shelf Life (2016). https://doi.org/10.1016/j.fpsl.2016.10.004
64. M.F.Z. Kadir, Ionics (2021). https://doi.org/10.1007/s11581-021-03992-4
65. J. Ahmed, M.Z. Mulla, Y.A. Arfat, Food Control (2016). https://doi.org/10.1016/j.foodcont.2016.05.013
66. H.S. Canbay, B. Bardakci, Süleyman Demirel Üniversitesi Fen Edebiyat Fakültesi Fen Dergisi **6**(2), 140–148 (2011)
67. W. Ma, C.H. Tang, S.W. Yin, X.Q. Yang, Q. Wang, F. Liu, Z.H. Wei, Food Res. Int. (2012). https://doi.org/10.1016/j.foodres.2012.07.037
68. M. Pirnia, K. Shirani, F.T. Yazdi, S.A. Moratazavi, M. Mohebbi, Food Chem. (2022). https://doi.org/10.1016/j.fochx.2022.100300
69. M. Ghasemlou, N. Aliheidari, R. Fahmi, S. Shojaee-Aliabadi, B. Keshavarz, M.J. Cran, R. Khaksar, Carbohydr. Polym. (2013). https://doi.org/10.1016/j.carbpol.2013.07.026